Quadrifilar Helical Antenna as a Whole-Body Traveling-Wave RF Coil for 3T and 7T MRI

Branislav M. Notaros[1], Milan M. Ilic[1], Alexey A. Tonyushkin[2], Nada J. Sekeljic[1], and Pranav Athalye[1]

[1]*Department of Electrical and Computer Engineering, Colorado State University, Fort Collins, Colorado, United States,* [2]*Radiology Dept., Massachusetts General Hospital, Harvard Medical School, Boston, Massachusetts, United States*

Introduction: The state-of-the-art traveling wave (TW) antennas as implemented in MRI systems at $B_0 \geq 7$ T include patch antennas that excite linear or circularly polarized (CP) TW fields inside a scanner's bore [1]. This excitation of TW, however, if not aided by additional electrodynamic elements (dielectrics or metamaterials), is highly localized, which results in rapid power dissipation in the body and thus in high local SAR levels in regions of the body and quick attenuation with distance away from the antenna. On the other hand, several recent attempts to improving homogeneity of whole-body coils in pre-clinical scanners at $B_0 > 3$ T include various modifications of near-field birdcage coils, such as spiral coils [2] that still operate in the near-field regime. Here we propose a novel method for TW-MRI at high- and ultra-high-fields (with $B_0 \geq 3$ T) using a bore-extended, subject-loaded helical antenna as a whole-body TW RF coil. The novel helical antenna RF coil has clear advantages over patch antennas, as well as over any other existing TW excitation methods and is simultaneously a solution for a whole-body RF coil at high fields.

Theory: Helical antennas, considered in their standard mode of operation, in free space, can be designed to radiate a right-hand CP endfire beam in the far field [3]. In addition, the main idea for our study is based on the fact that the helical antenna is essentially a TW antenna, and that the current along the wire of the antenna behaves like a traveling current wave. So the TW current of the helical antenna when placed in the MRI bore in Fig. 1 will radiate a TW $\mathbf{B}_1^+$ RF field into the subject inside it.

Methods: Modeling and analysis of the MRI structure in Fig. 1 are performed using a higher order full-wave computational electromagnetics (CEM) technique based on the method of moments (MoM) in conjunction with the surface integral equation (SIE) approach [4]. In addition, the results obtained by the higher order MoM-SIE technique are thoroughly verified and validated by comparison with results using two well-established commercial full-wave CEM codes, a MoM code WIPL-D and a finite element method (FEM) code ANSYS HFSS. Although monofilar and bifilar helical antennas are also possible choices, we propose here a quadrifilar helical antenna design, with four helices (Helices 1–4 in Fig. 1) wound coaxially and fed in time-phase quadrature, i.e., by 90° out of phase with respect to one another, against the common back plate, so their currents flow along the wires in time-phase quadrature. For most of our numerical simulations, we utilized the setup shown in Fig. 2: 3-T or 7-T MRI system with a standard clinical bore of diameter $D_B = 60$ cm and length $L_B = 200$ cm and a cylindrical phantom of diameter $D_p = 15$ cm and length $L_p = 100$ cm, with conical buffers of length $L_c = 28$ cm, filled with saline water of relative permittivity $\varepsilon_r = 81$ and conductivity $\sigma = 0.6$ S/m. The quadrifilar helical antenna of length $L_H = L_B = 200$ cm and wire diameter $d_w = 1$ cm is fed as in Fig. 1, against the back plate of diameter $D_B = 60$ cm, with $V = 1$ V RMS voltage at each excitation port.

Results and Discussion: Fig. 3 shows B_1^+ and B_1^- along the axis of the phantom in Fig. 2 at $B_0 = 3$ T and with helix diameter $D_H = 50$ cm and pitch $P = 12.8$ cm, where we observe a practically vanishing B_1^-, an excellent B_1^+/B_1^- ratio, and an excellent spatial uniformity of $\mathbf{B}_1^+$ along the axis. From cross-sectional field maps in Fig. 3, we observe an excellent B_1^+/B_1^- ratio and spatial uniformity of $\mathbf{B}_1^+$ throughout the entire phantom. Fig. 4 shows B_1^+ and B_1^- along the axis and the real part of the axial component of the Poynting vector in a longitudinal cross section of the phantom in Fig. 2 at $B_0 = 7$ T and with $D_H = 31$ cm and $P = 10.5$ cm, where an excellent B_1^+/B_1^- ratio and a very strong and uniform $\mathrm{Re}\{P_z\}$ and TW penetration in the entire phantom are observed. Fig. 5 shows B_1^+ and B_1^- along the axis of the human body model inside the helical antenna and the MRI bore (Fig. 1) at $B_0 = 3$ T, where we observe a very small B_1^- compared to B_1^+ everywhere except in the neck area ($z \approx 0.2$ m), where the B_1^+/B_1^- ratio can be improved if needed using a small collar-like absorber.

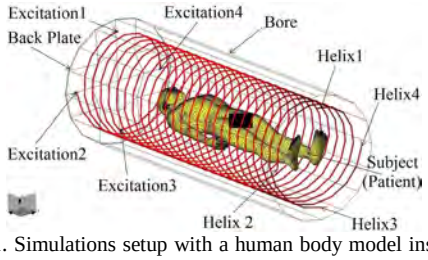

Fig. 1. Simulations setup with a human body model inside a TW quadrifilar helical antenna used as whole-body RF coil.

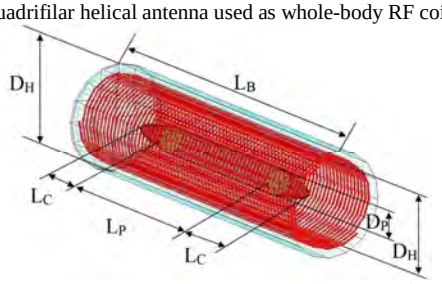

Fig. 2. Setup: 3-T or 7-T bore with an RF coil in the form of a bore-extended, phantom-loaded quadrifilar helical antenna.

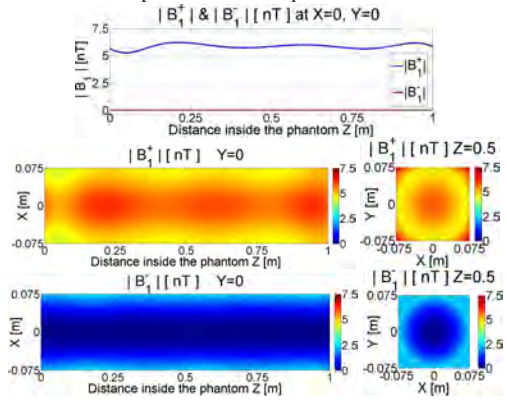

Fig. 3. Distributions of $\mathbf{B}_1^+$ and $\mathbf{B}_1^-$ along the axis and in longitudinal and transversal cross sections of the phantom in Fig. 2 at $B_0 = 3$ T ($f_0 = 127.8$ MHz).

Conclusions: Our full-wave CEM simulations of 3-T and 7-T MRI systems with bore-extended, phantom-loaded helical antennas (some of which are presented here) show (1) achieved TW regime at $B_0 = 3$ T, that is below normal frequency cut-off requirements without specially designed dielectrics; (2) excellent right-hand CP and B_1^+/B_1^- ratio throughout the phantoms; (3) high spatial uniformity of the $\mathbf{B}_1^+$ field throughout the phantoms; (4) efficient coupling of the wave with the subject; and (5) low SAR levels at every point in the phantom (body). Another feature of the novel TW whole-body RF coil is the simplicity of feed. In principle, our method for TW RF excitation is universal and not limited to any particular B_0 (f_0.) However, designs and demonstrations of whole-body helical antenna TW RF coils at fields other than 3 T and 7 T are yet to be done as part of our future work.

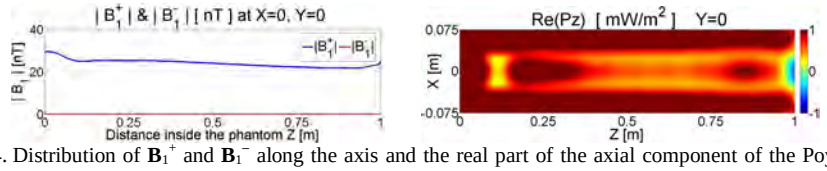

Fig. 4. Distribution of $\mathbf{B}_1^+$ and $\mathbf{B}_1^-$ along the axis and the real part of the axial component of the Poynting vector in a longitudinal cross section of the phantom in Fig. 2 at $B_0 = 7$ T ($f_0 = 300$ MHz).

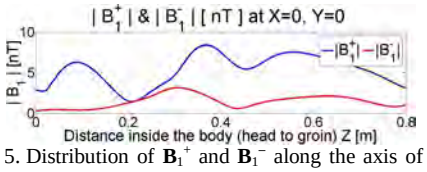

Fig. 5. Distribution of $\mathbf{B}_1^+$ and $\mathbf{B}_1^-$ along the axis of the human body model in Fig. 1; $B_0 = 3$ T ($f_0 = 127.8$ MHz).

References: [1] Zhang B, et al. Design of a patch antenna for creating traveling waves at 7 Tesla. Proc.17th ISMRM 2009:4746. [2] Alsop D, et al. A spiral volume coil for improved RF field homogeneity at high static magnetic field strength. Magn Reson Med. 1998;40:49-54. [3] Djordjević A R, et al. Optimization of Helical Antennas. IEEE Antennas Propagat. Magazine. 2006;48(6):107-115. [4] Djordjevic M and Notaros B M, Double higher order method of moments for surface integral equation modeling of metallic and dielectric antennas and scatterers. IEEE Trans Antennas Propagat. 2004;52(8):2118-2129.